한국해양공학회지 제20권 6호, pp 7~17 2006년 12월 (ISSN 1225-0767)

Controller Design for an Autonomous Underwater Vehicle Using Estimated Hydrodynamic Coefficients

JOON-YOUNG KIM*
*College of Ocean Sciences, Cheju National University, Jeju, Korea

KEY WORDS: Autonomous underwater vehicle (AUV), Hydrodynamic coefficients, Extended kalman filter, Sliding mode observer, Sliding mode control

ABSTRACT: *Depth and heading control of an AUV are considered to follow the predetermined depth and heading angle. The proposed control algorithm is designed. based on a sliding mode control using estimated hydrodynamic coefficients. The hydrodynamic coefficients are estimated with conventional nonlinear observer techniques, such as sliding mode observer and extended Kalman filter. By using the estimated coefficients, a sliding mode controller is constructed for the combined diving and steering maneuver. The simulation results of the proposed control system are compared with those of control system with true coefficients. This paper demonstrates the proposed control system, discusses the mechanisms that make the system stable and follows the desired depth and heading angle, accurately, in the presence of parameter uncertainty.*

1. Introduction

In recent years, intensive efforts have been concerted towards the development of autonomous underwater vehicles (AUVs). In order to design an AUV, it is usually necessary to analyze its maneuverability and controllability, based on a mathematical model. The mathematical model for most 6 DOF contains hydrodynamic forces and moments expressed in terms of a set of hydrodynamic coefficients. Therefore, in order to simulate the performance of the AUV correctly, it is important to know the true values of these coefficients.

The hydrodynamic coefficients constitute the heart of the primary mathematical model used in simulation studies of rigid-body motions of AUVs. These coefficients are usually considered constant, independent of vehicle motion parameters. A number of mathematical models have been developed, particularly for AUVs, where the number and type of hydrodynamic coefficients are different, depending on the modeling of the forces and moments, e.g., the quadratic form, the cubic form, and the combined quadratic-cubic form for damping forces and moments. The various hydrodynamic coefficients appearing in the dynamic equations of motion may be classified into 3 types, such as the added mass coefficients, due to the inertia of the surrounding fluid, and the linear/nonlinear damping coefficients, which result from fluid viscosity effects. Among these, the linear damping coefficients have the largest affect on the maneuverability of an AUV (Sen, 2000). Sen (2000) examined the influence of various hydrodynamic coefficients on the predicted maneuverability quality of submerged bodies and found that the coefficients with significant effects on the trajectories are the linear damping coefficients.

These coefficients are normally obtained by experimental test, numerical analysis or empirical formula. Although the planar motion mechanism (PMM) test is the most popular among experimental tests, the measured values are not completely reliable because of experimental difficulties and errors.

Another approach is the observer method, which estimates the hydrodynamic coefficients with the help of a model-based estimation algorithm. A representative method among observer methods is the Kalman filter, which has been widely used in the estimation of hydrodynamic coefficients and state variables. Hwang (1980), Kim (1996), and Yoon (2003) estimated the maneuvering coefficients of a ship and identified the dynamic system of a maneuvering ship, using an extended Kalman filtering technique.

These estimated coefficients are not only used for a mathematical model to analyze AUV's maneuvering performance, but also for a controller model to design an AUV's autopilot. Antonelli et al. (2000) estimated a vehicle-manipulator system's velocity using observer and applied it in tracking control law. Fossen and Blanke

교신저자 김준영: 제주시 제주대학로 66번지
064-754-3485 jkim@cheju.ac.kr

(2000) designed a propeller shaft speed controller by using feedback from the axial water velocity in the propeller disc. Farrell and Clauberg (1993) reported successful control of the Sea Squirt vehicle, which used an extended Kalman filter as a parameter estimator with pole placement to design the controller. Yuh (1990) has described the functional form of vehicle dynamic equations of motion, the nature of the loadings, and the use of adaptive control via online parameter identification.

Recently, advanced control techniques have been developed for AUVs, aimed at improving the capability to track the desired position and attitude trajectories. In particular, sliding mode control has been successfully applied to AUV because of good robustness for modeling uncertainty, variation from operating condition, and disturbance. Yoerger and Slotine (1985) proposed a series of SISO continuous-time controllers by using the sliding mode technique on an underwater vehicle, and demonstrated the robustness of their control system by computer simulation in the presence of parameter uncertainties. Cristi et al. (1990) proposed an adaptive sliding mode controller for AUVs, based on the dominant linear model and the bounds of the nonlinear dynamic perturbations. Healey and Lienard (1993) and Sur and Seo (1992) described a 6 DOF model for the maneuvering of an underwater vehicle and designed a sliding mode autopilot for the combined steering, diving, and speed control functions. Lea et al. (1999) compared the performance of root locus, fuzzy logic, and sliding mode control, and tested them using an experimental vehicle. Lee et al. (1998) designed a quasi-sliding mode controller for an AUV in the presence of parameter uncertainties and a long sampling interval.

In this paper, depth and heading control of an AUV are presented in order to maintain the desired depth and heading angle in a towing tank. The proposed control algorithm represents a sliding mode control using the estimated hydrodynamic coefficients. The hydrodynamic coefficients are estimated, based on the nonlinear observer such as sliding mode observer (SMO) and extended Kalman filter (EKF). Because the system to be controlled is highly nonlinear, a sliding mode control is constructed to compensate for the effects of modeling nonlinearity, parameter uncertainty, and disturbance.

This paper is organized as follows.: Section 2 describes the nonlinear observers for estimating the hydrodynamic coefficients. Section 3 presents a sliding mode control for depth and heading control. Section 4 shows simulation results. Finally, section 5 presents the conclusions.

2. Estimation of the Hydrodynamic Coefficients

The coefficients with the most significant effects on the dynamic performance of an AUV are found to be the linear damping coefficients. In particular, ten coefficients among the linear damping coefficients are considered as highly sensitive parameters and represented in Sen (2000) as M_q, M_{ds}, N_r, N_{dr}, N_v, Z_{ds}, Z_q, Y_{dr}, Y_r, and Y_v.

In this paper, in order to estimate the sensitive coefficients, the estimate system based on a nonlinear observer is constructed, as illustrated in Fig. 1. The nonlinear observer block is composed of SMO and EKF, which are designed based on the AUV's 6 DOF equations of motion. Based on the measured signal of the AUV's motion, two nonlinear observers are developed for estimating the sensitive coefficients. The AUV block represents the real plant and includes a 6 DOF model of NPS AUV II (Healey and Lienard, 1993). The value of the sensitive coefficients from this block is used as the true value and compared with the estimated ones.

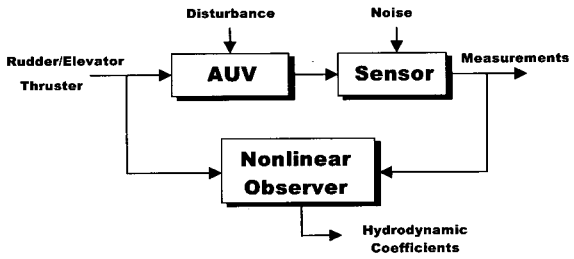

Fig. 1 Configuration of the estimate system

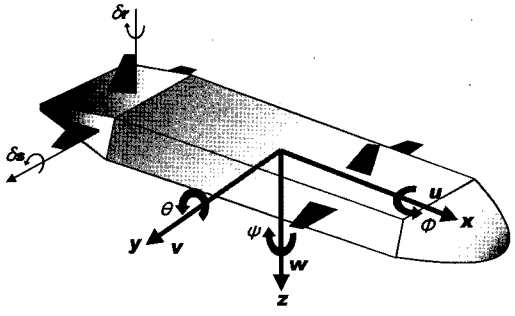

Fig. 2 Coordinate system

In nonlinear observers, 6 DOF AUV equations of motion and the augmented states for the linear damping coefficients are included. Thus, the observer model describes surge, sway, heave, roll, pitch, and yaw motions. The coordinate system is shown in Fig. 2. The 6 DOF equations of motion for the observer design are as follows (Fossen, 1994):

$$\begin{aligned}
&m[\dot{u}-vr+wq-x_G(q^2+r^2)+y_G(pq-\dot{r})+z_G(pr+\dot{q})]=X\\
&m[\dot{v}+ur-wp+x_G(pq+\dot{r})-y_G(p^2+r^2)+z_G(qr-\dot{p})]=Y\\
&m[\dot{w}-uq+vp+x_G(pr-\dot{q})+y_G(qr+\dot{p})-z_G(p^2+q^2)]=Z\\
&I_x\dot{p}+(I_z-I_y)qr+I_{xy}(pr-\dot{q})-I_{yz}(q^2-r^2)-I_{xz}(pq+\dot{r})\\
&\qquad +m[y_G(\dot{w}-uq+vp)-z_G(\dot{v}+ur-wp)]=K\\
&I_y\dot{q}+(I_x-I_z)pr-I_{xy}(qr+\dot{p})+I_{yz}(pq-\dot{r})+I_{xz}(p^2-r^2)\\
&\qquad -m[x_G(\dot{w}-uq+vp)-z_G(\dot{u}-vr+wq)]=M\\
&I_z\dot{r}+(I_y-I_x)pq-I_{xy}(p^2-q^2)-I_{yz}(pr+\dot{q})+I_{xz}(qr-\dot{p})\\
&\qquad +m[x_G(\dot{v}+ur-wp)-y_G(\dot{u}-vr+wq)]=N
\end{aligned} \tag{1}$$

where u, v, and w are the velocities of surge, sway, and heave motion, and p, q, and r are the angular velocities of roll, pitch, and yaw motion, respectively. X, Y, Z, K, M, and N represent the resultant forces and moments with respect to x, y, and z axis, respectively; their detailed expressions and nomenclatures are described in Fossen (1994). In order to estimate the linear damping coefficients, they have to be modeled as extra state variables. Consequently, Eq. (1), the 6 DOF equations of motion, is transformed into augmented state-space form as follows:

$$[M]\begin{bmatrix}\dot{u}\\ \dot{v}\\ \dot{w}\\ \dot{p}\\ \dot{q}\\ \dot{r}\\ \dot{\phi}\\ \dot{\theta}\\ \dot{\psi}\\ \dot{\xi}\end{bmatrix}=\begin{bmatrix}X_e+X_m\\ Y_e+Y_m\\ Z_e+Z_m\\ K_e+K_m\\ M_e+M_m\\ N_e+N_m\\ p+q\sin\phi\tan\theta+r\cos\phi\tan\theta\\ q\cos\phi-r\sin\phi\\ (q\sin\phi+r\cos\phi)\sec\theta\\ 0\end{bmatrix} \tag{2}$$

where $M\in R^{19\times 19}$ is the inertia matrix with hydrodynamic added mass, and the extra state $\xi\in R^{10\times 1}$ denotes the linear damping coefficients. ϕ, θ, and ψ are the angles of roll, pitch, and yaw, respectively. X_e, Y_e, Z_e, K_e, M_e, and N_e represent the external forces and moments, except the added mass term. X_m, Y_m, Z_m, K_m, M_m, and N_m stand for the components of the inertial terms transposed from the left hand-side of Eq. (1). The detailed expressions are shown in the Appendix. Especially, the added mass coefficients and the nonlinear damping coefficients in Eq. (2) are taken from NPS AUV II (Healey and Lienard, 1993) as known values. Therefore, nonlinear observers are designed based on Eq. (2).

2.1 Sliding mode observer (SMO)

The SMO, which is developed on the basis of the sliding surface concept, can set the gain value according to the uncertainty range of the plant model. The SMO is known to be robust under parameter uncertainty and disturbance. In addition, it can be easily applied to the nonlinear system (Slotine et al., 1987). In general, a nonlinear system may be represented by:

$$\begin{aligned}\dot{x}&=f(x,t)\\ y&=Cx\end{aligned} \tag{3}$$

where $x\in R^n$ is the state vector, $y\in R^m$ is the measurement vector, $f(x,t)$ is the true plant and $C\in R^{m\times n}$ is the measurement matrix. The measurement is assumed to be a linear combination of the state, and the inputs are contained in $f(x,t)$. If we define a sliding surface s as the error $\tilde{y}$,

$$s=\tilde{y}=\hat{y}-y=C(\hat{x}-x) \tag{4}$$

then, the sliding surface converges to zero when it satisfies the Lyapunov stability, as follows:

$$s\dot{s}=\tilde{y}\dot{\tilde{y}}<0 \tag{5}$$

Eq. (5) is referred to as the sliding condition. If Eq. (5) is satisfied, the sliding surface $s=0$ is guaranteed and the error $\tilde{y}$ tends toward zero. In order to satisfy the sliding condition, the SMO is given by:

$$\dot{\hat{x}}=f(\hat{x},t)-L\tanh(\tilde{y}/\Phi) \tag{6}$$

where L is the nonlinear gain matrix to be determined and $tanh(\tilde{y}/\Phi)$ represents the switching term, which uses the 'tanh' function, instead of 'sign' function. Φ is

the boundary layer thickness, and it acts as a low-pass filter to remove chattering and noise. From Eq. (3) and Eq. (6), the error dynamics is given by:

$$\begin{aligned}\dot{\tilde{x}} &= \dot{\hat{x}} - \dot{x} \\ &= f(\hat{x},t) - f(x,t) - L\tanh(\tilde{y}/\Phi) \\ &= \Delta f(\tilde{x},t) - L\tanh(\tilde{y}/\Phi)\end{aligned} \tag{7}$$

where $f(\hat{x},t)$ is the modeled plant. The value of $\triangle f(\tilde{x},t)$ depends both on the modeling complexity and on the error magnitude. Using the error dynamics, Eq. (7), the sliding condition is as follows:

$$\tilde{y}\dot{\tilde{y}} = \tilde{y}C\dot{\tilde{x}} = \tilde{y}C(\Delta f - L\tanh(\tilde{y}/\Phi)) < 0 \tag{8}$$

To satisfy Eq. (8), given bounds on $\triangle f$, the nonlinear gain L is chosen by:

$$L_i > |\Delta f_i(\tilde{x},t)| \quad , \quad (i = 1 \sim p) \tag{9}$$

Here L_i is pth order nonlinear gain. In addition, during sliding, namely when the sliding surface goes to zero, the switching term can be written from Eq. (8).

$$\tanh(\tilde{y}/\Phi) \approx (CL)^{-1}C\Delta f \tag{10}$$

From Eq. (10), the error dynamics Eq. (7) is developed given by:

$$\dot{\tilde{x}} \approx [I - L(CL)^{-1}C]\Delta f \tag{11}$$

where I implies the identity matrix. Therefore, the system dynamics are reduced from nth order to the n-pth order during sliding. The above Eq. (11) has the form of $\dot{\tilde{x}} = \alpha\tilde{x}$; so, the nonlinear gain matrix L is chosen, such that α has a negative eigenvalue.

In order to estimate the hydrodynamic coefficients, the SMO is designed using the observer model Eq. (2). The state variable yields to $x = [u\ v\ w\ p\ q\ r\ \phi\ \theta\ \psi\ M_q\ M_{ds}\ N_r\ N_{dr}\ N_v\ Z_{ds}\ Z_q\ Y_{dr}\ Y_r\ Y_v]^T$. The output variables are chosen as $y = [u\ v\ w\ p\ q\ r\ \phi\ \theta\ \psi]^T$.

2.2 Extended kalman filter (EKF)

The EKF can estimate the state variables optimally in nonlinear stochastic cases that include plant perturbation and sensor noise. In particular, unknown inputs or parameters can be estimated by converting them to extra state variables (Ray, 1995). Assume that a system that contains unknown parameters is given as follows:

$$\begin{aligned}x_{k+1} &= f(x_k, \xi_k, k) + w_k \\ y_k &= h(x_k, \xi_k, k) + v_k\end{aligned} \tag{12}$$

where $x \in R^n$ is the state vector, $y \in R^m$ is the measurement vector, $\xi \in R^p$ is the unknown parameter vector, w is the plant disturbance, and v is the sensor noise. In order to estimate the unknown parameters, the state variable x is augmented by the unknown parameters. Therefore, Eq. (12) can be expressed in augmented state-space form as follows:

$$\begin{aligned}x^*_{k+1} &= \begin{bmatrix} x_{k+1} \\ \xi_{k+1} \end{bmatrix} = \begin{bmatrix} f(x_k, \xi_k, k) \\ 0 \end{bmatrix} + \begin{bmatrix} w_k \\ \eta_k \end{bmatrix} \\ y_k &= h(x^*_k, k) + v_k\end{aligned} \tag{13}$$

where $w \in R^n$, $\eta \in R^p$ and $v \in R^m$ are zero-mean Gaussian white noise sequences and $x^* \in R^{n+p}$ is the augmented state vector. For this system, the discrete time EKF is summarized as:

Time update:

$$\hat{x}^*_{k+1}(-) = f(\hat{x}^*_k(+), k) \tag{14}$$

$$P_{k+1}(-) = F^*_k P_k(+) F^{*T}_k + Q_k \tag{15}$$

Measurement update:

$$K_k = P_k(-) H^{*T}_k \left[H^*_k P_k(-) H^{*T}_k + R_k \right]^{-1} \tag{16}$$

$$\hat{x}^*_k(+) = \hat{x}^*_k(-) + K_k \left[y_k - h(\hat{x}^*_k(-), k) \right] \tag{17}$$

$$P_k(+) = \left[I - K_k H^*_k \right] P_k(-) \tag{18}$$

where $F^*_k = \left.\dfrac{\partial f(x^*,k)}{\partial x^*}\right|_{x^* = \hat{x}^*_k(+)}$, $H^*_k = \left.\dfrac{\partial h(x^*,k)}{\partial x^*}\right|_{x^* = \hat{x}^*_k(-)}$

P is the error covariance and Q is the process noise covariance. The gain matrix K is determined from the Riccati equation, and the measurement noise covariance R is determined by satisfying the Lyapunov function of error (Boutayeb et al., 1997). P and Q are determined by scaling the fixed magnitude (Kim, 1999). Time

updates Eq. (14) and Eq. (15) mean extrapolation by state transition matrix and measurement updates Eq. (16), Eq. (17) and Eq. (18) reflect the actual measurement process by optimal gain K.

To estimate the hydrodynamic coefficients, the EKF is designed using the observer model of Eq. (2). The 10 linear damping coefficients, which are represented by ξ, are estimated through Eqs. (14)~(18). The state and output variables are equal to those of the SMO.

2.3 Estimation results

In order to estimate the ten sensitive coefficients associated with horizontal and vertical motions, simulation is conducted for combined diving and steering motion of the AUV. The sensitive coefficients from the AUV block in Fig. 1 are used as true values and compared with the estimated ones. The estimation performance of the SMO and the EKF is compared when the AUV undergoes combined diving and steering. The motion scenario is as follows: the AUV has the initial speed of 1.8 m/sec and the rudder/elevator angle is applied to 20° from the start. The rudder and elevator works within -23° to 23°. Figures 3 shows the rudder/elevator angles, the velocities and the 3-D trajectory of the motion scenario.

Figures 4~7 compare the estimation results of the SMO and the EKF for the ten sensitive coefficients. The steady-state error is compared in Table 1. In the figures, a thick solid line represents the true value adopted from Healey and Lienard (1993), and the dashed/solid line represents the SMO/EKF result. In general, the EKF shows a good estimation performance, but Y_{dr}, Y_r, and Y_v, which are associated with sway motion, have steady-state error. It is well known that the SMO is a robust observer under parameter uncertainty and disturbance, but it has a large steady-state error and fluctuation at the transient period. Based on a series of simulations, it is concluded that the EKF estimates the sensitive coefficients with sufficient accuracy. Although the nonlinear observers have been used off-line in order to analyze system identification, those can be implemented on-line for estimating the state variables and control of an AUV.

In this paper, nonlinear observers for estimating the hydrodynamic coefficients represent a good performance because input data for the observer are taken from simulation results of NPS AUV II. However, it is expected that the estimated coefficients contains a lot of

Table 1 Steady-state error (%)

	SMO	EKF
M_q	1.10	0.12
M_{ds}	1.46	0.26
N_r	24.67	0.33
N_{dr}	17.78	0.58
N_v	30.35	0.13
Z_{ds}	3.07	0.05
Z_q	2.48	0.09
Y_{dr}	49.34	14.53
Y_r	102.57	9.61
Y_v	44.22	23.29

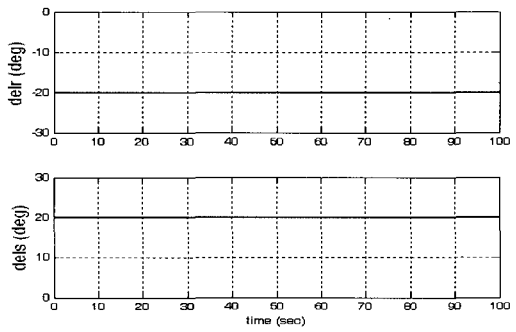

(a) Steering and elevator angles

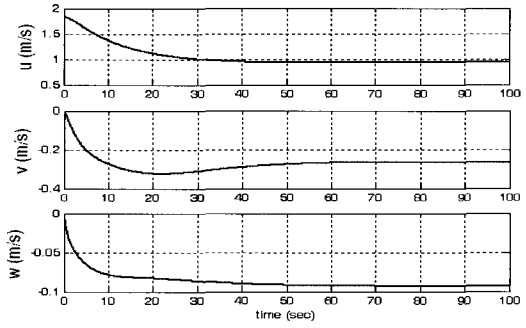

(b) Surge, sway, and heave velocities

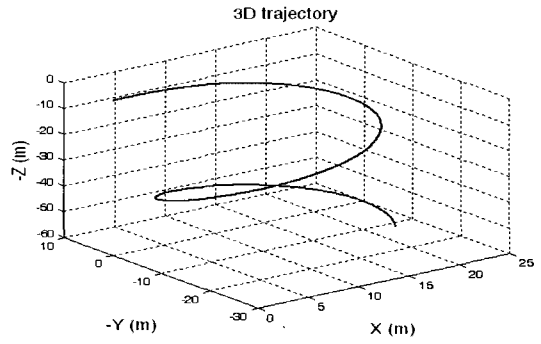

(c) 3-D trajectory

Fig. 3 Inputs and outputs of motion scenario

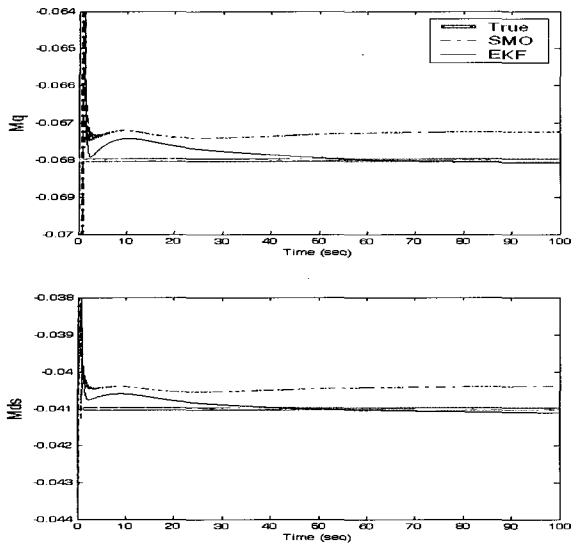

Fig. 4 Pitch coefficients M_q and M_{ds}

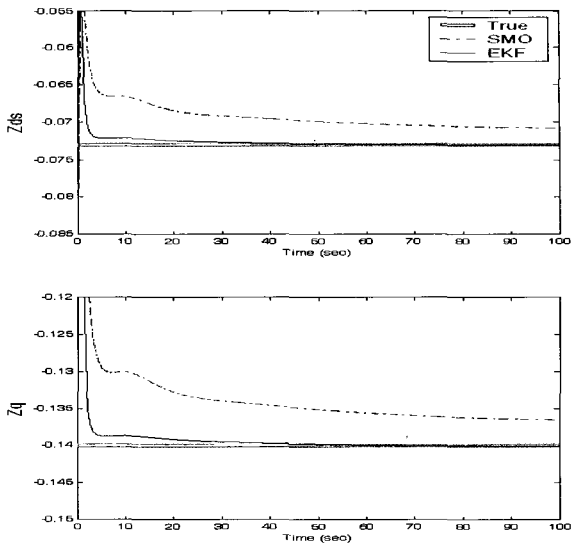

Fig. 6 Heave coefficients Z_{ds} and Z_q

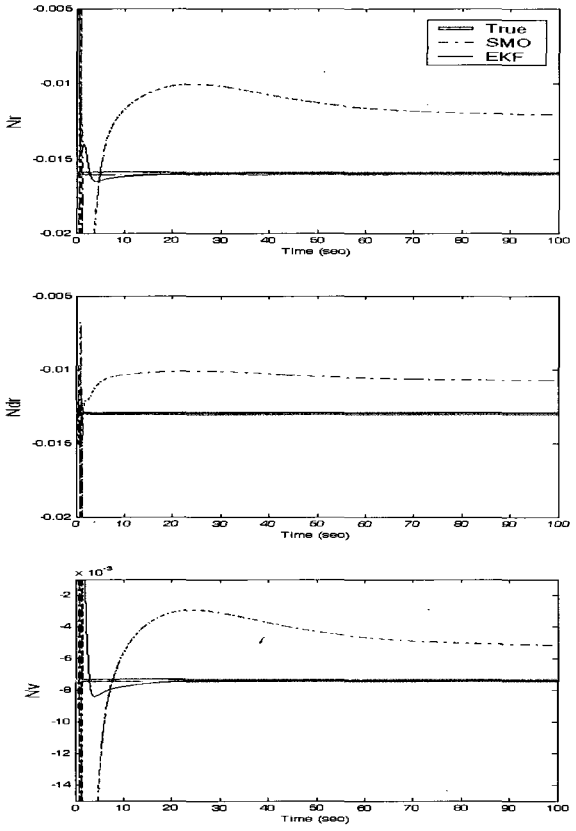

Fig. 5 Yaw coefficients N_r, N_{dr} and N_v

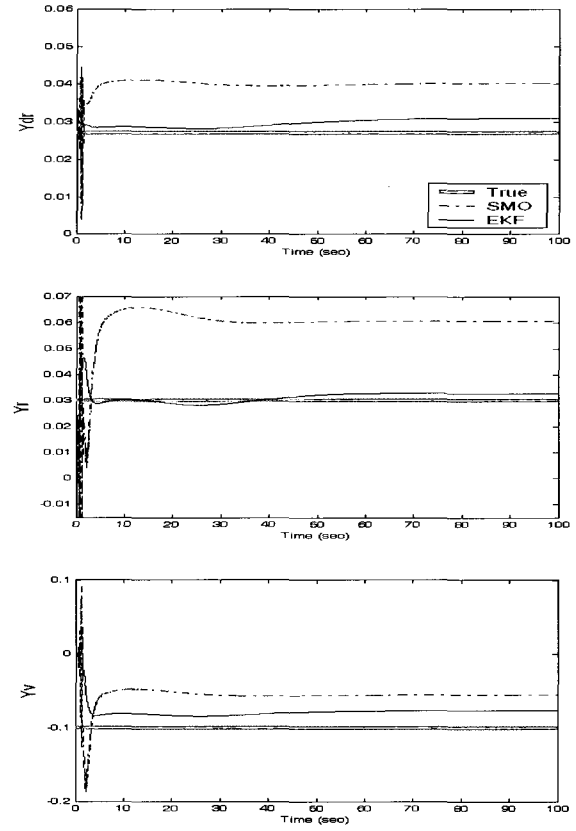

Fig. 7 Sway coefficients Y_{dr}, Y_r and Y_v

errors when the input data are taken from sea trial results. The sea trial data can be contaminated with sensor noise and contain complex terms caused by coupled motion of an AUV.

3. Controller Design

Although an AUV system is difficult to control, due to high nonlinearity and motion coupling, sliding mode

control has been successfully applied to underwater vehicles. In this paper, a sliding mode control is adopted for an AUV with the uncertainty of system parameters. Particularly, when designing a sliding mode controller, the estimated hydrodynamic coefficients in section 2 are applied in the controller model.

It is well known that the sliding mode control provides an effective and robust way of controlling uncertain plants by means of a switching control law, which drives the plant's state trajectory onto the sliding surface in the state space. With only a single control element active, each subsystem may be treated separately as a single input, multi-state system with its own single sliding surface definition. Any system is described as a single input, multi-state equation (Healey and Lienard, 1993).

$$\begin{aligned} &\dot{x(t)} = Ax(t) + bu(t) + \delta f(t) \\ &x(t) \in R^{n\times 1},\ A \in R^{n\times n}, b \in R^{n\times 1} \end{aligned} \tag{19}$$

where $\delta f(t)$ is a nonlinear function, describing disturbances and unmodelled coupling effects. The sliding surface is defined as:

$$\sigma = s^T \tilde{x} \tag{20}$$

where s^T represents the sliding surface coefficient and $\tilde{x}$ the state error, *i.e.* $\tilde{x} = x - x_d$. It is important that the sliding surface is defined such that as the sliding surface tends toward zero, the state error also tends toward zero. Sliding surface reaches zero in a finite amount of time by the condition:

$$\dot{\sigma} = -\eta sgn(\sigma) \tag{21}$$

where η represents nonlinear switching gain. From Eq. (19) and Eq. (21), we obtain

$$s^T(Ax + bu + \delta f - \dot{x}_d = -\eta sgn(\sigma) \tag{22}$$

and control input is determined as follows:

$$u = -(s^T b)^{-1} s^T Ax + (s^T b)^{-1}[-s^T \delta f + s^T \dot{x}_d - \eta sgn(\sigma)] \tag{23}$$

If the pair (A,b) is controllable and $(s^T b)$ is nonzero, then it may be shown that the sliding surface coefficients are the elements of the left eigenvector of the closed-loop dynamics matrix $(A - bk^T)$ corresponding to a pole at the origin

$$s^T[A - bk^T] = 0 \tag{24}$$

where the linear gain vector, k^T, is defined $(s^T b)^{-1} s^T A$ and can be evaluated from the standard method, such as pole placement. It should be mentioned that one of the eigenvalues of $(A - bk^T)$ must be specified to be zero. The resulting sliding control law, using a *'tanh'* function, is given as:

$$u = -k^T x - (s^T b)^{-1} s^T \delta f + (s^T b)^{-1} s^T \dot{x} - \eta (s^T b)^{-1} \tanh(\sigma/\Phi) \tag{25}$$

where Φ is the boundary layer thickness and it acts as a low-pass filter to remove chattering and noise. The choice of the nonlinear switching gain, η, and the boundary layer thickness, Φ, is selected to eliminate control chattering.

3.1 Depth control

In order to design a controller in the vertical plane, the linearized diving system dynamics are developed as follows:

$$\begin{aligned} (I_y - \frac{\rho}{2} L^5 M_{\dot{q}})\dot{q} &= (\frac{\rho}{2} L^4 u \widehat{M}_q) q - (z_G - z_B) W\theta \\ &\quad + (\frac{\rho}{2} L^3 u^2 \widehat{M}_{\delta s}) \delta_s \\ \dot{\theta} &= q \\ \dot{Z} &= -u\theta \end{aligned} \tag{26}$$

In Eq. (26), the values of $\hat{M}_q$ and $\hat{M}_{\delta s}$ are taken from the estimated ones (EKF) in section 2. Then, the dynamic model for depth control yields the state equation as:

$$\begin{bmatrix} \dot{q} \\ \dot{\theta} \\ \dot{Z} \end{bmatrix} = \begin{bmatrix} -1.002 & -0.066 & 0 \\ 1 & 0 & 0 \\ 0 & -1.8320 & 0 \end{bmatrix} \begin{bmatrix} q \\ \theta \\ Z \end{bmatrix} + \begin{bmatrix} -0.209 \\ 0 \\ 0 \end{bmatrix} \delta_s \tag{27}$$

The sliding surface is defined as

$$\sigma_s = 28.18\tilde{q} + 14.37\tilde{\theta} - \tilde{Z} \tag{28}$$

where $\tilde{q}$, $\tilde{\theta}$, and $\tilde{Z}$ represent the errors of pitch rate,

pitch angle, and depth, respectively. When the poles are placed at [0 -0.25 -0.26]. Finally, the depth control law is determined as:

$$\delta_s = 2.3531q + 0.0062\theta - 0.1698\dot{Z}_d + 2.3\tanh(\sigma_s/4) \quad (29)$$

For implementation of the above depth control law, an AUV has to be equipped with the pitch rate, pitch angle, and depth sensors.

3.2 Heading control

The linearized steering system dynamics are given as follows:

$$\begin{aligned}(m-\frac{\rho}{2}L^3Y_{\dot{v}})\dot{v} - (\frac{\rho}{2}L^4Y_{\dot{r}})\dot{r} &= (\frac{\rho}{2}L^2u\hat{Y}_v)v + (\frac{\rho}{2}L^3u\hat{Y}_r - mu)r \\ &\quad + (\frac{\rho}{2}L^2u^2\hat{Y}_{\delta r})\delta_r \\ -(\frac{\rho}{2}L^4N_{\dot{v}})\dot{v} + (I_z - \frac{\rho}{2}L^5N_{\dot{r}})\dot{r} &= (\frac{\rho}{2}L^3u\hat{N}_v)v + (\frac{\rho}{2}L^4u\hat{N}_r)r \\ &\quad + (\frac{\rho}{2}L^3u^2\hat{N}_{\delta r})\delta_r\end{aligned}$$

$$\dot{\psi} = r \quad (30)$$

In Eq. (30), the values of $\hat{Y}_v, \hat{Y}_r, \hat{Y}_{\delta r}, \hat{N}_v, \hat{N}_r$, and $\hat{N}_{\delta r}$ are taken from the estimated ones (EKF). Then, the dynamic model for heading control yields the state equation as:

$$\begin{bmatrix}\dot{v}\\ \dot{r}\\ \dot{\psi}\end{bmatrix} = \begin{bmatrix}-0.209 & -0.605 & 0\\ -0.054 & -0.569 & 0\\ 0 & 1 & 0\end{bmatrix}\begin{bmatrix}v\\ r\\ \psi\end{bmatrix} + \begin{bmatrix}0.145\\ -0.152\\ 0\end{bmatrix}\delta_r \quad (31)$$

The values to place the poles of the steering system at [0 -0.41 -0.42] become

$$\sigma_r = 0.15\tilde{v} + 1.65\tilde{r} + \tilde{\psi} \quad (32)$$

where $\tilde{v}$, $\tilde{r}$, and $\tilde{\psi}$ denote the errors of sway velocity, yaw rate, and yaw angle, respectively. The heading control law is as follows:

$$\delta_r = 0.5260v + 0.1621r + 4.3465\dot{\psi}_d + 1.5\tanh(\sigma_r/0.05) \quad (33)$$

In order to implement the above heading control law, it is necessary to measure the signals of lateral velocity, yaw rate, and yaw angle.

4. Simulation Results

Numerical simulations have been performed in order to show the effectiveness of the proposed control system. The simulation program, which is developed using MATLAB 6.0 with SIMULINK 4.0 environment, is shown in Fig. 8. The controller block is composed of a sliding mode controller and a PID controller for the depth and heading control. The AUV data of input and output, as the true plant, are taken from NPS AUV II (Healey and Lienard, 1993). The depth and heading controls are simulated with the full nonlinear equation and the sliding mode controller developed in Eq. (29) and Eq. (33). The responses of control law with the EKF values, which are nearly the same as the true ones, are compared with those of control law with the SMO values that contain steady-state errors.

In addition, the performance of the sliding mode controller is compared with that of the PID controller. It is well known that the traditional PID controller with fixed gains can not meet the requirements of underwater vehicle control. However, the traditional PID controller and the modified PID controller with variable gains are applied for an AUV in the field.

Figure 9 shows the desired depth, tracking trajectory, and other controlled variables for the depth control simulation, which is carried out with the heading control to avoid the horizontal motion due to coupling. The desired depth is 1 m down from the initial depth, during the first 50 secs, and then it resumes to the initial depth thereafter. From these figures, it is found that the performance of the controller with the SMO is similar to that of the controller with the EKF. The controller with the SMO has a particularly good tracking performance, despite the coefficients' deviations.

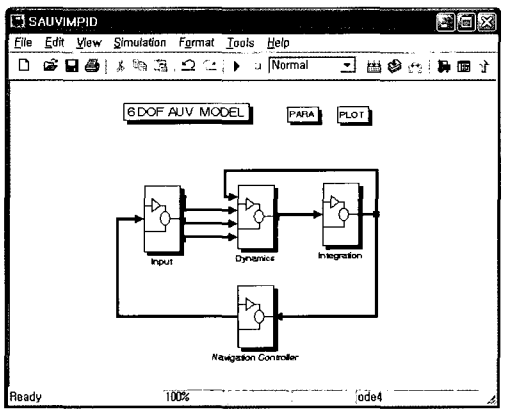

Fig. 8 SIMULINK model for control simulation

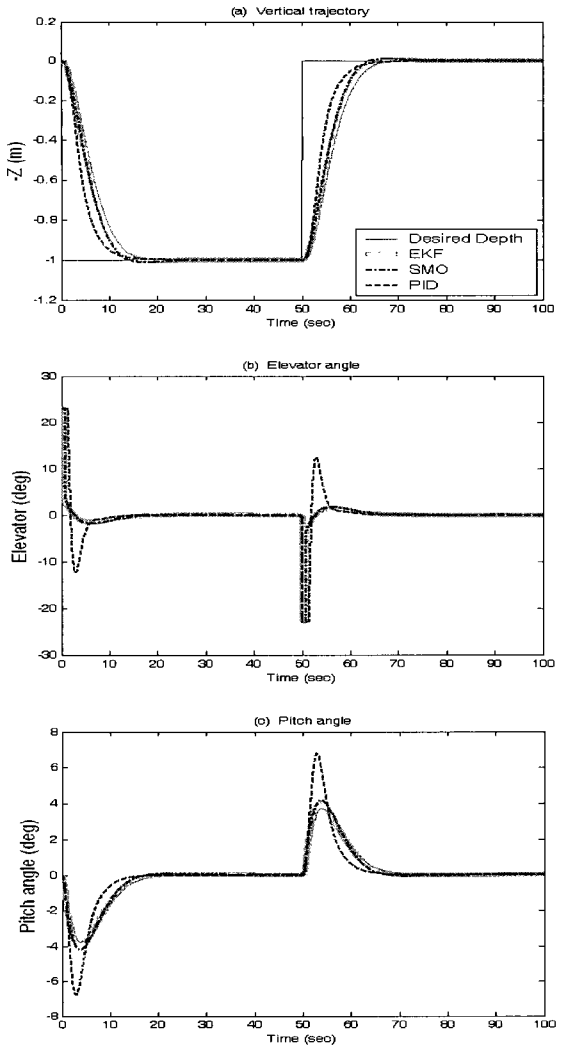

Fig. 9 Simulation results of depth control

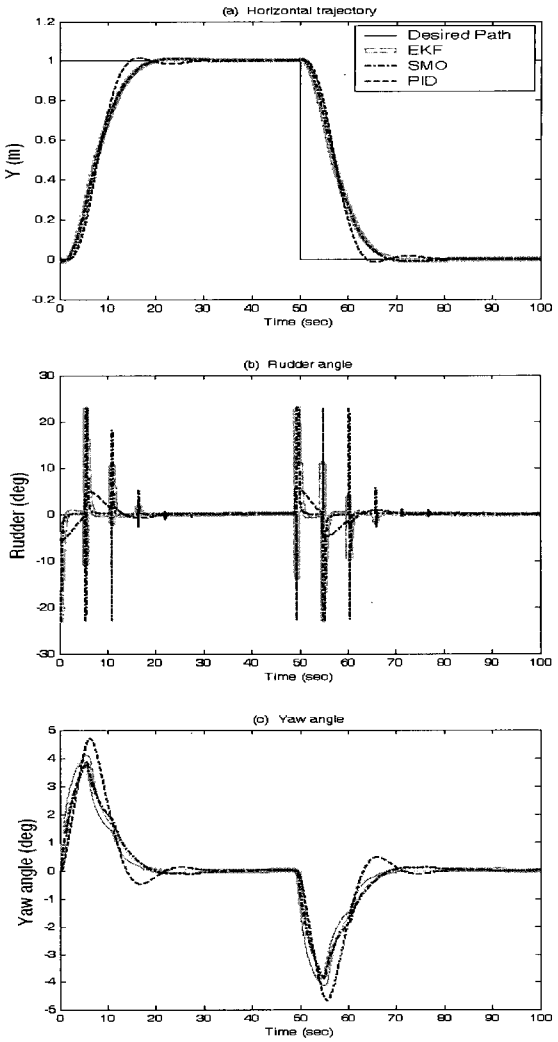

Fig. 10 Simulation results of heading control

This result means that the sliding mode control is robust, even under parameter uncertainty. In addition, the performance of the controller with nonlinear observer is similar to that of the PID controller.

Figure 10 shows the responses of the heading control. The heading control is simulated with depth control to prevent the vertical motion due to coupling. To follow the desired path, we define the line of sight (Healey and Lienard, 1993) in terms of a desired yaw angle, and then the proposed heading control follows the desired yaw angle. The desired path is chosen 1 m towards the y-direction, during the first 50 secs, and then returned to the initial position. In the figures, the controller with the SMO follows the desired path, similar to that of the controller with the EKF, but the controller with the SMO needs a little more rudder angle, as seen in Fig. 10 (b). It is worth noting that the controller with the SMO follows the desired path, even when the estimated coefficients contain some steady-state errors.

5. Conclusions

A sliding mode control using the estimated hydrodynamic coefficients is proposed in this paper to maintain the desired depth and heading angle. The hydrodynamic coefficients are estimated, based on the nonlinear observers of SMO and EKF. The EKF has a particularly good estimation performance and estimates the coefficients with sufficient accuracy, although it has some steady-state errors. Using the estimated coefficients, a sliding mode controller is designed for the diving and steering maneuver. The control system with the SMO is compared to the control system with

the EKF. It is demonstrated that the proposed control system is stable and accurately follows the desired depth and path. It means that the sliding mode control shows the robustness under parameter uncertainties. The proposed estimation method is believed to reduce the PMM test for measuring the hydrodynamic coefficients. In addition, the proposed control system makes the AUV stable and controllable in the presence of parameter uncertainties.

Acknowledgements

This work was supported by the Korea Research Foundation Grant funded by the Korean Government (MOEHRD). (KRF-2003- 214-D00149)

References

Antonelli, G., Caccavale, F., Chiaverini, S. and Villani, L. (2000). "Tracking Control for Underwater Vehicle-Manipulator Systems with Velocity Estimation", IEEE J. of Oceanic Eng., Vol 25, No 3, pp 399-413.

Boutayeb, M., Rafaralahy, H. and Darouach, M. (1997). "Convergence Analysis of the Extended Kalman Filter Used as an Observer for Nonlinear Deterministic Discrete-Time Systems", IEEE Trans. on Autom. Control, Vol 42, No 4, pp 581-586.

Cristi, R., Papoulias, F.A. and Healey, A.J. (1990). "Adaptive Sliding Mode Control of Autonomous Underwater Vehicles in the Dive Plane", IEEE J. of Oceanic Eng., Vol 15, No 3, pp 152-160.

Farrell, J. and Clauberg, B. (1993) "Issues in the Implementation of an Indirect Adaptive Control System", IEEE J. of Oceanic Eng., Vol 18, No 3, pp 311-318.

Fossen, T.I. (1994). Guidance and Control of Ocean Vehicles, John Wiley & Sons.

Fossen, T.I. and Blanke, M. (2000). "Nonlinear Output Feedback Control of Underwater Vehicle Propellers Using Feedback from Estimated Axial Flow Velocity", IEEE J. of Oceanic Eng., Vol 25, No 2, pp 241-255.

Healey, A.J. and Lienard, D. (1993). "Multivariable Sliding Mode Control for Autonomous Diving and Steering of Unmanned Underwater Vehicles", IEEE J. of Oceanic Eng., Vol 18, No 3, pp 327-339.

Hwang, W.Y. (1980). Application of System Identification to Ship Maneuvering, Ph.D. Thesis, MIT.

Kim, C.K. (1996). Estimation of Manoeuvring Coefficients of a Submerged Body by Parameter Identification, Ph.D. Thesis, Seoul National University.

Kim, J.Y. (1999). Development of Tire Force Monitoring Systems Using Nonlinear Observers, Ph.D. Thesis, Hanyang University.

Lea, R.K., Allen, R. and Merry, S.L. (1999). "A Comparative Study of Control Techniques for an Underwater Flight Vehicle", International J. of System Science, Vol 30, No 9, pp 947-964.

Lee, P.M., Jeon, B.H. and Hong, S.W. (1998). "Quasi-Sliding Mode Control of an Autonomous Underwater Vehicle with Long Sampling Interval", J. of Ocean Engineering and Technology Eng., Vol 12, No 2, pp 130-138.

Masmoudi, R.A. and Hedrick, J.K. (1992). "Estimation of Vehicle Shaft Torque Using Nonlinear Observers", ASME J. of Dynamics, Measurement, and Control, Vol 114, pp 394-400.

Ray, L.R. (1995). "Stochastic Decision and Control Parameters for IVHS", ASME IMECE Advanced Automotive Technologies, pp 114-118.

Sen, D. (2000). "A Study on Sensitivity of Maneuverability Performance on the Hydrodynamic Coefficients for Submerged Bodies", J. of Ship Research, Vol 44, No 3, pp 186-196.

Slotine, J.J.E., Hedrick, J.K. and Misawa, E.A. (1987). "On Sliding Observers for Nonlinear Systems", ASME J. of Dynamics, Measurement, and Control, Vol 109, pp 245-252.

Sur, J.N. and Seo, Y.T. (1992). "Design and Experimental Evaluation of Sliding Mode Controller for Nonlinear Autonomous Underwater Vehicle", J. of Ocean Engineering and Technology, Vol 6, No 1, pp 11-18.

Yoerger, D.R. and Slotine, J.J.E. (1985). "Robust Trajectory Control of Underwater Vehicles", IEEE J. of Oceanic Eng., Vol OE-10, No 4, pp 462-470.

Yoon, H.K. (2003). Estimation of Hydrodynamic Coefficients Using the Estimation-Before-Modeling Technique, Ph.D. Thesis, Seoul National University.

Yuh, J. (1990). "Modeling and Control of Underwater Vehicles", IEEE Trans. on Syst,, Man, Cybern., Vol 20, pp 1475-1483.

Appendix

$$M=\begin{bmatrix} m-\frac{\rho}{2}L^3X_{\dot{u}} & 0 & 0 & 0 & mz_G & 0 & \vdots & \\ 0 & m-\frac{\rho}{2}L^3Y_{\dot{v}} & 0 & -mz_G-\frac{\rho}{2}L^4Y_{\dot{p}} & 0 & -\frac{\rho}{2}L^4Y_{\dot{r}} & \vdots & \\ 0 & 0 & m-\frac{\rho}{2}L^3Z_{\dot{w}} & 0 & -\frac{\rho}{2}L^4Z_{\dot{q}} & 0 & \vdots & \\ 0 & -mz_G-\frac{\rho}{2}L^4K_{\dot{v}} & 0 & I_x-\frac{\rho}{2}L^5K_{\dot{p}} & -I_{xy} & -I_{xz}-\frac{\rho}{2}L^5K_{\dot{r}} & \vdots & 0_{6\times13} \\ mz_G & 0 & -\frac{\rho}{2}L^4M_{\dot{w}} & -I_{xy} & I_y-\frac{\rho}{2}L^5M_{\dot{q}} & -I_{yz} & \vdots & \\ 0 & -\frac{\rho}{2}L^4N_{\dot{v}} & 0 & -I_{xz}-\frac{\rho}{2}L^5N_{\dot{p}} & -I_{yz} & I_z-\frac{\rho}{2}L^5N_{\dot{r}} & \vdots & \\ \cdots & \cdots & \cdots & \cdots & \cdots & \cdots & \cdots & \cdots \\ & & & 0_{13\times6} & & & \vdots & I_{13\times13} \end{bmatrix}$$

$$\begin{aligned}
X_e &= \frac{\rho}{2}L^4\left[X_{pp}p^2+X_{qq}q^2+X_{rr}r^2+X_{pr}pr\right]+\frac{\rho}{2}L^3\left[X_{wq}wq+X_{vp}vp+X_{vr}vr+X_{q\delta s}uq\delta_s+X_{r\delta r}ur\delta_r\right] \\
&\quad+\frac{\rho}{2}L^2\left[X_{vv}v^2+X_{ww}w^2+X_{v\delta r}uv\delta_r+X_{w\delta s}uw\delta_s+u^2(X_{\delta s\delta s}\delta_s^2+X_{\delta r\delta r}\delta_r^2)\right] \\
&\quad-(W-B)\sin\theta+\frac{\rho}{2}L^3X_{q\delta sn}uq\delta_s\varepsilon(n)+\frac{\rho}{2}L^2\left[X_{\delta s\delta sn}u^2\delta_s^2\right]\varepsilon(n)+\frac{\rho}{2}L^2u^2X_{prop} \\
Y_e &= \frac{\rho}{2}L^4\left[Y_{pq}pq+Y_{qr}qr\right]+\frac{\rho}{2}L^3\left[Y_pup+Y_rur+Y_{vq}vq+Y_{wp}wp+Y_{wr}wr\right] \\
&\quad+\frac{\rho}{2}L^2\left[Y_vuv+Y_{vw}vw+Y_{\delta r}u^2\delta_r\right]+(W-B)\cos\theta\sin\phi \\
Z_e &= \frac{\rho}{2}L^4\left[Z_{pp}p^2+Z_{pr}pr+Z_{rr}r^2\right]+\frac{\rho}{2}L^3\left[Z_quq+Z_{vp}vp+Z_{vr}vr\right]+\frac{\rho}{2}L^2\left[Z_wuw+Z_{vv}v^2+Z_{\delta s}u^2\delta_s\right] \\
&\quad+(W-B)\cos\theta\cos\phi+\frac{\rho}{2}L^3Z_{qn}uq\varepsilon(n)+\frac{\rho}{2}L^2\left[Z_{wn}uw+Z_{\delta sn}u^2\delta_s\right]\varepsilon(n) \\
K_e &= \frac{\rho}{2}L^5\left[K_{pq}pq+K_{qr}qr\right]+\frac{\rho}{2}L^4\left[K_pup+K_rur+K_{vq}vq+K_{wp}wp+K_{wr}wr\right]+\frac{\rho}{2}L^3\left[K_vuv+K_{vw}vw\right] \\
&\quad+(y_GW-y_BB)\cos\theta\cos\phi-(z_GW-z_BB)\cos\theta\sin\phi+\frac{\rho}{2}L^4K_{pn}up\varepsilon(n)+\frac{\rho}{2}L^3u^3K_{prop} \\
M_e &= \frac{\rho}{2}L^5\left[M_{pp}p^2+M_{pr}pr+M_{rr}r^2\right]+\frac{\rho}{2}L^4\left[M_quq+M_{vp}vp+M_{vr}vr\right]+\frac{\rho}{2}L^3\left[M_wuw+M_{vv}v^2+M_{\delta s}u^2\delta_s\right] \\
&\quad-(x_GW-x_BB)\cos\theta\cos\phi-(z_GW-z_BB)\sin\theta+\frac{\rho}{2}L^4M_{qn}uq\varepsilon(n)+\frac{\rho}{2}L^3\left[M_{wn}uw+M_{\delta sn}u^2\delta_s\right]\varepsilon(n) \\
N_e &= \frac{\rho}{2}L^5\left[N_{pq}pq+N_{qr}qr\right]+\frac{\rho}{2}L^4\left[N_pup+N_rur+N_{vq}vq+N_{wp}wp+N_{wr}wr\right]+\frac{\rho}{2}L^3\left[N_vuv+N_{vw}vw+N_{\delta r}u^2\delta_r\right] \\
&\quad+(x_GW-x_BB)\cos\theta\sin\phi+(y_GW-y_BB)\sin\theta+\frac{\rho}{2}L^3u^2N_{prop}
\end{aligned}$$

$$\begin{aligned}
X_m &= m[vr-wq+x_G(q^2+r^2)-y_Gpq-z_Gpr] \\
Y_m &= -m[ur-wp+x_Gpq-y_G(p^2+r^2)+z_Gqr] \\
Z_m &= m[uq-vp-x_Gpr-y_Gqr+z_G(p^2+q^2)] \\
K_m &= -(I_z-I_y)qr-I_{xy}pr+I_{yz}(q^2-r^2)+I_{xz}pq-m[y_G(vp-uq)-z_G(ur-wp)] \\
M_m &= -(I_x-I_z)pr+I_{xy}qr-I_{yz}pq-I_{xz}(p^2-r^2)+m[x_G(vp-uq)-z_G(wq-vr)] \\
N_m &= -(I_y-I_x)pq+I_{xy}(p^2-q^2)+I_{yz}pr-I_{xz}qr-m[x_G(ur-wp)-y_G(wq-vr)]
\end{aligned}$$

2006년 5월 2일 원고 접수
2006년 11월 15일 최종 수정본 채택